INVESTIGATION ON THE EFFECTS OF HUMAN WEIGHT ON INTERVERTEBRAL DISC AT HUMAN LUMBAR SPINE USING FINITE ELEMENT ANALYSIS

TAN KAH YIN

This report is submitted
in fulfillment of the requirement for the degree of
Bachelor of Mechanical Engineering (Structure and Material)

Faculty of Mechanical Engineering

UNIVERSITI TEKNIKAL MALAYSIA MELAKA

MAY 2017

SUPERVISOR'S DECLARATION

I have checked this report and the report can now be submitted to JK-PSM to be delivered back to supervisor and to the second examiner.

Signature : ....

Name of Supervisor: ....

Date : ....

DECLARATION

I declare that this project report entitled "Investigation On The Effects Of Human Weight On Intervertebral Disc At Human Lumbar Spine Using Finite Element Analysis" is the result of my own work except as cited in the references.

Signature	: ....
Name	: ....
Date	: ....

ABSTRACT

The population of obesity is expected to increase especially in developed country. The excess human weight compared to normal weight produce extra force to the lumbar spine .Therefore, the increased load originated from the human weight change the mechanical properties of the intervertebral disc which can lead to damage in nucleus pulposus and annulus fibrosus. However, this project intended to investigate the biomechanical effect of human weight on intervertebral disc at human lumbar spine using finite element analysis. The compressive load of 700 N, 900 N and 1100 N with flexion and extension were exerted to the human lumbar spine model that represent the population of normal, overweight and obese. From the result obtained from ABAQUS, the pressure and stress distribution in intervertebral disc increases from normal to obese compressive load. The highest pressure in nucleus pulposus obtained from the analysis was 2.7 MPa during extension motion in L2-L3 lumbar segment under obese compressive load tended to cause disc degeneration disease. Additionally, the highest percentage difference of annulus stress distribution resulted 108.12 % compared to normal weight load during flexion motion in L2-L3 lumbar segment. This increasing weight condition elevated the risk for annulus fibrosus to rupture and damage.

ABSTRAK

Populasi obesiti dijangka akan meningkat terutamanya di negara maju. Keberatan manusia yang berlebihan berbanding dengan keberatan badan biasa menghasilkan daya tambahan di tulang belakang lumbar. Oleh itu, peningkatan beban yang berasal daripada keberatan badan manusia akan mengubah sifat-sifat mekanikal cakera intervertebral yang akan merosakan pulposus nukleus dan anulus fibrosus. Selain itu, tujuan projeck ini adalah untuk menyiasat kesan biomekanik kepelbagaian keberatan manusia pada cakera intervertebral di tulang belakang lumbar manusia menggunakan analisis unsur terhingga. Beban mampatan sebanyak 700 N, 900 N dan 1100 N dengan kombinasi aksi akhiran dan lanjutan telah dikenakan pada model tulang belakang lumbar manusia yang mewakili populasi normal, berat badan berlebihan dan obes. Keputusan yang diperolehi dalam ABAQUS menunjukkan kenaikan taburan tekanan dan tekanan dalam cakera intervertebral dari normal kepada beban mampatan obes. Tekanan tertinggi di pulposus nukleus diperolehi daripada analisis adalah 2.7 MPa semasa lanjutan gerakan dalam L2-L3 segmen lumbar bawah beban mampatan gemuk cenderung untuk menyebabkan penyakit degenerasi cakera. Selain itu, perbezaan peratusan tertinggi agihan tegasan anulus sebanyak 108.12% tinggi berbanding dengan beban berat badan normal semasa akhiran gerakan dalam L2-L3 segmen lumbar. keadaan berat badan yang semakin meningkat ini meninggikan risiko untuk merosakkan and memecahkan anulus fibrosus.

ACKNOWLEDGEMENT

First, I would like to thank project supervisor Dr. Mohd Juzaila bin Abd Latif for guiding me during this two semester. Furthermore, I would also like to thank to my fellow friends who support me during this period throughout this studies.

TABLE OF CONTENTS

LIST OF TABLE

LIST OF FIGURES

LIST OF APPENDICES

LIST OF ABBREVIATION

FEM	Finite element method
LBP	Low back pain
DDD	Degenerated discs disease
IVD	Intervertebral disc
AF	Annulus fibrosus
NP	Nucleus pulposus
L1	The first lumbar vertebra
L2	The second lumbar vertebra
L3	The third lumbar vertebra
L4	The fourth lumbar vertebra
L5	The fifth lumbar vertebra
FEA	Finite element analysis
TDR	Total disc displacement
UTM	Universiti Teknologi Malaysia
FE	Finite element
ROM	Range of motion

IDP	Intradiscal pressure
PLL	Posterior longitudinal ligament
ALL	Anterior longitudinal ligament
LF	Ligamentum flavum
CL	Capsular ligament
ITL	Intertransverse ligament
ISL	Interspinous ligament
SSL	Supraspinous ligament
OA	Osteoarthritis

LIST OF SYMBOLS

E	-	Yong’s modulus
v	-	Poisson’s ratio
C_1, C_2	-	Material constant characterising the deviataric deformation
M	-	Moment
F	-	Force
d	-	Displacement

CHAPTER 1

INTRODUCTION

1.1 Background

Low back pain (LBP) is one of the public health disorder experienced by human race and it is reported to be 75 % of the population in developed countries experience this musculoskeletal disorder (Viera 2008). Moreover, it threats the health care system and socioeconomics of the countries (Koh et al. 2010). Simplistic, the uncomfortable pain faced by the patient will affect their life quality and daily activities such as climbing, pulling, pushing and lifting or running.

Degeneration Disc Disease (DDD) is declared as the trigger of LBP (Smith et al. 2011). The DDD is originated from the losses of water content and crack condition of IVD tend to reduce its strength to absorb external stresses (Unal et al. 2011). Therefore, the biomechanical behavior changes in IVD maneuver the severity of DDD.

The intervertebral discs (IVD) is a fibrocartilage consist of annulus fibrosus (AF) and a centrally located nucleus pulposes (NP) that can withstand and support the loads from internal and external (O'Connell et al. 2011). Dehydration in the IVDs are known as degenerative disc disease will change the mechanical properties of the IVD and result in structural failure as time goes by (Smith et al. 2011).

Generally, the probability of vertebral to be damaged is depend on the IVD health condition which has the ability to distribute compressive load from human weight (Hussein et al. 2013). However, the attention of this project is to focus on the relationship between the human weights on the biomechanical effect of lumbar spine.

Likewise, the model of the lumbar spine (L1-L5) is constructed using CAD software and the model is simulated by implementing finite element analysis (FEA) which is one of the computational technique to estimate and anticipate the effect of weight on the lumbar spine. The FEA software is worth to be implemented as the results from the simulation can be obtained precisely, faster and economically.

Occasionally, the kinematic motions of the healthy lumbar spine model in flexion, extension, lateral bending, and axial rotation are vitally important to be determined as it will influenced the mechanical properties of the intervertebral disc (Denoziere & Ku 2006). Therefore, this project seems vitally essential as the result obtained are practicable and fabrication of artificial IVD for total disc replacement (TDR) will be more accurate.

1.2 Problem statement

The expanding numbers of obesity and overweight population currently seem to become the norm in the country like China and United State will worsen the severity of the LBP in the nation (Porto et al. 2012; Gordon-Larsen et al. 2014). One of the causes of the LBP is DDD as the mass of water content in IVD decreases via DDD. However, the heavier human weight tends to weaken the strength of disc to withstand the compressive loads and tensile stresses (Silva & Claro 2015).Therefore, it is extremely important to investigate the biomechanical effect of human weight on the disc using FEA of various BMI.

1.3 Objectives

The specific objectives of this project are as follows:

1) To develop a finite element model of the lumbar spine.
2) To investigate the biomechanical effects of IVD at various human weight using FEA.

1.4 Scope

The original three dimensional (3D) model of L1 to L5 lumbar spine was obtained from UTM Faculty of Bioscience and Medical Engineering for simulation purposes. The L1-L5 lumbar spine model was developed and simulated using ABAQUS. The ligaments were neglected in the simulation. The biomechanical effects of normal weight, overweight and obesity were focused on the IVD with intradiscal pressure and von-Mises stress.

CHAPRER 2

LITERATURE REVIEW

2.1 Overview

This chapter describes the background of LBP and human lumbar spine. The development of the FE model of human lumbar spine shows significant effect in future research in mitigating the problems faced by the actual human lumbar spine.

2.2 Spine biomechanics

Biomechanics of the spine define the movement pattern of human spine that causes by force in the body structure. It exposes the functions and principles of the vertebral structures, tissues, ligaments and discs in providing spine stability. Generally, the kinematic and dynamic stability of human spine depend on the motion and muscle. The validation of the mechanical stability will be failed if the muscle or motion is not considered in the human spine simulation and experiments (Bergmark 1989). Therefore, any misunderstanding and misconception of biomechanics of the spine will lead to nervous system damages.

The kinematic motions of the spine can be divided into extension, flexion, and lateral bending as shown in Figure 2.1. This motions are capable to influence the biomechanical effect of the lumbar spine under certain loads (Wong et al. 2003; Panjabi et al. 1994).

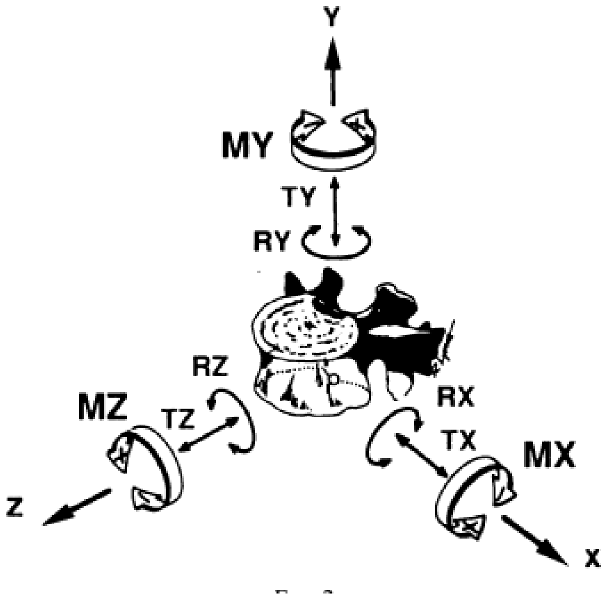

Figure 2.1 The 3D coordinate system used to describe lateral bending (MZ), axial rotation (MY), extension and flexion (MX). Adapted from Panjabi et al. (1994).

2.3 Anatomy of the human spine

The best way to know the function of lumbar spine is to understand the structure and components in the spine. The structure of the human spine can be simplified into five region which is cervical, thoracic, lumbar, sacrum and coccyx region as shown as Figure 2.2.

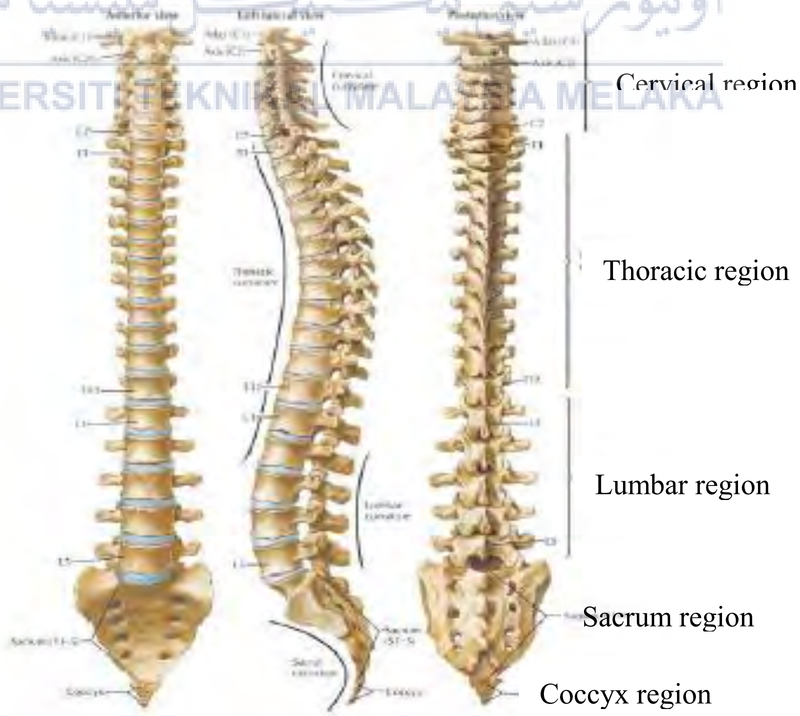

Figure 2.2 Cervical, thoracic, lumbar, sacrum and coccyx regions of the human spine. Adapted from Aleti & Motaleb (2014).

The cervical spine is comprises of seven vertebrae from C1-C7. Furthermore, the thoracic region is the combination of 12 vertebrae from T1-T12 and the lumbar spine contains 5 vertebrae from L1-L5. Likewise, the region of sacrum and coccyx contain 5 and 4 fused vertebrae. The curve shape and structure of the human spine enhance the mechanical flexibility and act as a shock absorber to support the body (Kurtz & Edidin 2006). This combination of regions ensure the spine is maintained in the stable state during walking, climbing, lifting, pulling, pushing and running.

2.4 Human lumbar spine

The main function of human lumbar spine is to withstand the weight of the upper body and maintain the extensibility and stability of the body in daily activities (Han et al. 2011). Nevertheless, the human lumbar spine is located between the thoracic and sacrum region and comprises of five rigid vertebrae connect with each other via facet joints and IVDs was shown in Figure 2.3. Additionally, the human lumbar spine is made up of vertebral body, posterior element, facet joints, intervertebral discs, ligaments, muscles and motion segments (Kurutz M. 2010).

Figure 2.3 The model of lumbar spine. Adapted from Netter (2006).

2.4.1 Lumbar vertebrae body

The vertebral body of the lumbar spine is comprises of thicker or denser and strong cortical bone on the outside and relatively thin cancellous bone on the inside of the vertebrae (Denoziere & Ku 2006). Moreover, the cancellous bone can be classified as porous biomaterials that create sponge-like network due to the horizontal and vertical struts reinforcement as shown in Figure 2.4 (Netter 2006).

Figure 2.4 The illustration of cancellous bone and cortical shell. Adapted from Netter (2006).

The natural process of human such as aging tends to change the morphological structure and reduce the density of bone mineral (Ferguson & Steffen 2003). Otherwise, the flexible characteristic of cancellous bone enhance the ability for vertebrae body to avoid large deformation in shape. Therefore, the interaction between the IVD and vertebrae body will be affected when loadings are apply in the lumbar spine region (White & Panjabi 1990).

2.4.2 Intervertebral disc

The IVD is a soft tissue that has high water content and assumed to be incompressible. It is located between two adjacent vertebras body and act as shock absorber when the external loads are acting on it was shown in Figure 2.5. Generally, the IVD contributes approximately 25 % of the spinal column height (Adam 2004). Since it is a shock absorber, ability to sustain sudden loads has become the key function of IVD in lumbar spine.

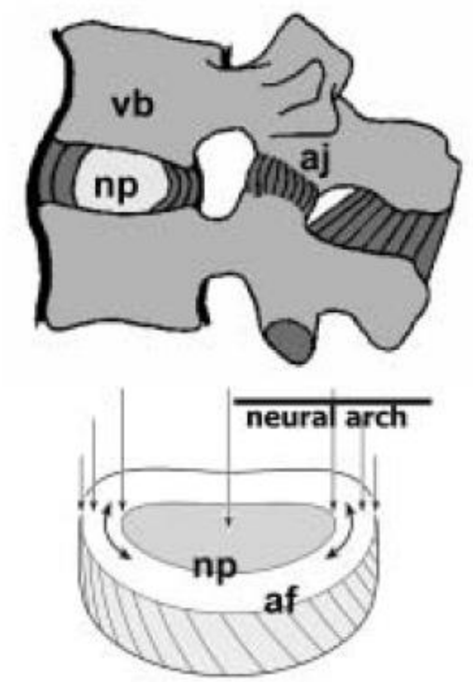

Figure 2.5 The upper image shows the location of IVD between two adjacent vetebrae and ligament. The lower image illustrates the structure of IVD comprises of NP and AF. Adapted from Adam (2004).

The IVD is comprised of nucleus pulposus (NP) and annulus fibrosus (AF) which lie at the center and outside portion of IVD (Khan et al. 2012). Therefore, the increases in body weight will vastly rise the magnitude of distribution load in the IVD and leads to decrease in height and volume of IVD (Araujo et al. 2015). Likewise, the Young modulus (E) and Poisson's ratio (ʋ) are the most crucial parameter in the disc's mechanical properties when assigning the value in the healthy disc model during finite element simulation (Khalaf et al. 2015). Otherwise, the hyperelastic behavior of IVD in term of Mooney-Rivlin concept can be assigned in the simulation to obtain better validation result (Schmidt et al. 2007). Moreover, this study aims to analyze the biomechanical behavior of healthy IVD under body weight from normal, overweight and obesity population.

2.4.3 Facet joint

The spinal facet joint is called as Zygapohyseal is located at the spinal column to link the vertebra together as shown in Figure 2.6. It is comprised of different type of soft and hard tissue that can reduce the friction when the lumbar spine is exerted by different loading direction (Jaumard et al. 2011).

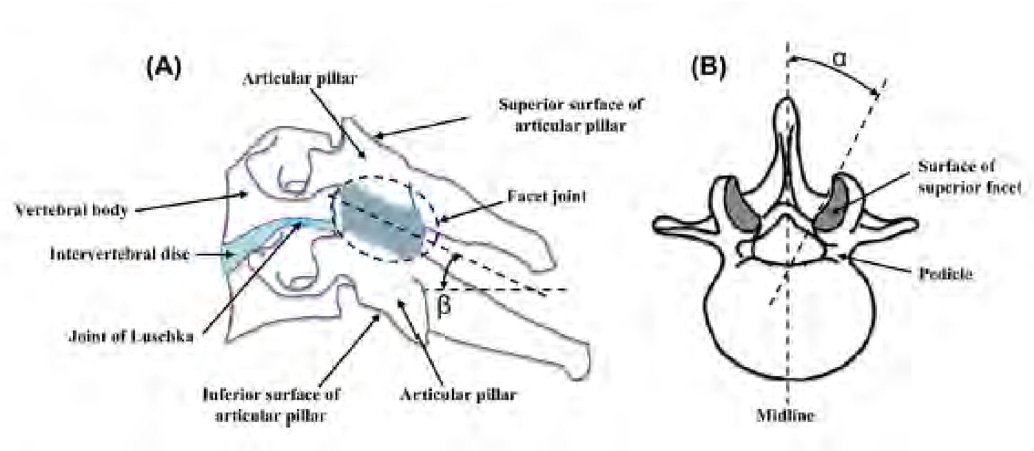

Figure 2.6 (a) Lateral view and (b) transverse view of facet joint in lumbar spine (Jaumard et al. 2011).

The changes of mechanical properties of facet joint tends to weaken the lubricant effect will lead to LBP. Therefore, the changes in flexibility of the lumbar spine will affect the range of motion verification of the model (Panjabi et al. 1994). The loading amount of 10% to 40% in the lumbar spine can be tranmitted to facet joint via various spine posture (Nabhani & Wake 2002).

2.4.4 Ligaments

There are seven ligament link to the lumbar spine, which are anterior longitudinal ligament (ALL), posterior longitudinal ligament (PLL), ligamentous flava (LF), supraspinal ligament (SSL), interspinous ligament (ISL), capsular ligament (CL) and intertransverse ligament (ITL) as shown in Figure 2.7.

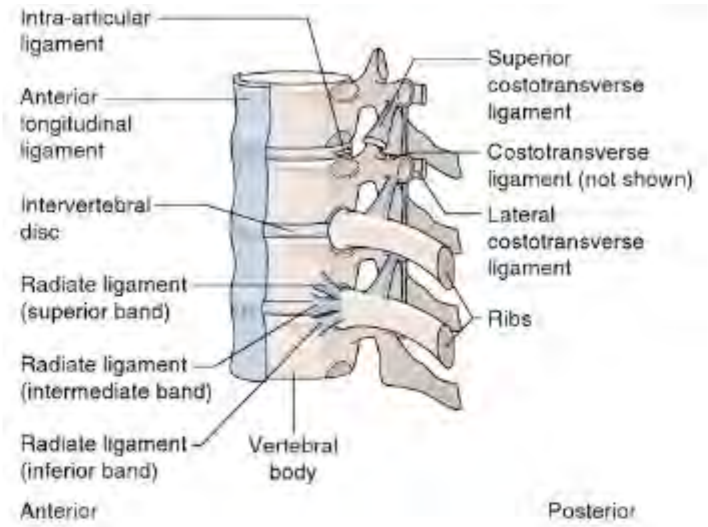

Figure 2.7 The ligaments existed in the lumbar spine. Adapted from Loudon (2012).

The ligaments constructed in the lumbar spine model are assumed to be in tension not pressure and their mechanical behavior is assignment during simulation state as shown as Table 2.1.

Table 2.1 The material porperties of ligaments. Adapted from Yu (2015)

Ligaments name	MOE/MPa	Poisson ratio	Sectional surface	Units
ALL	20	0.3	75.9	4
PLL	20	0.3	75.9	4
LF	19.5	0.3	8.7	2
SSL	11.6	0.3	75.7	1
ISL	15	0.3	6.1	4
CL	32.9	0.3	102.5	6

2.5 Low back pain

Generally, the normal human is declared as LBP patient once the trunk feel pain for six week continuously (Koes et al. 2006). LBP tends to limit the mobility of the patients due to the instability of the lumbar spine (Panjabi 2003). There are various causes of LBP such as smoking, aging, genetic, working environment and others. Likewise, the most common cause of LBP originates from degeneration of IVD (Shiri et al. 2010). Furthermore, the heavier spinal load originated from muscular force, height and weight worsen the severity of disc degeneration and decreases the intersegmental rotation of normal lumbar spine or contributes to spinal instability (Fujiwara et al.2000; Han et al. 2011).

2.5.1 Obesity

The increasing population of overweight and obesity tend to worsen the severity of low back pain worldwide (Porto et al. 2012). Likewise, recent studies indicate obesity population has higher risk to face LBP and leg pain compared to normal weight population (Djurasovic et al. 2008). The continuously trend of overweight and obesity population show significant effect in rising risk of disc degeneration via Magnetic Resonance imaging (Vismara et al. 2010). The loading condition of lumbar spine which comprises of muscle effect has the linearly behavior against body height and weight or BMI (Han et al. 2011). Therefore, the simulation of various human weight at constant height on the FE lumbar spine is vitally important in predicting the outcomes of various load to decrease the musculoskeletal pain (Martin et al. 2001).

2.5.2 Intervertebral disc degeneration

Degenerated discs diseases (DDD) means at least one of the IVD between two adjacent vetebrea unable to distribute the load normally as severe dehydration occurs in nuclues propulsus (NP) and annulus fibrosus (AF) (Tashtoush 2015). When the severity of dehydration reaches optimum level, the NP losses the ability to distribute the compressive load consistently to the AF. However, the water loss in nucleus reduce the height and mechanical properties of IVD tend to influence the biomechanics behaviour of lumbar spine (Smith et al. 2011; Park et al. 2013). Normally, the FE model of various severity level of IVD in human lumbar spine is fully simulated to obtained intersegmental rotation of lumbar spine, intradiscal pressure of IVD and force in facet joints (Park et al. 2013). Additionally, recent FE studies indicated the flexion motion of lumbar spine created greatest IDP in the degenerated disc (Schmidt et al. 2007).

2.6 Computational Method

The FEM is the technique frequently implemented in the industry in mitigating complex problem in the structure and design that cannot be solved using fundamental theories. Generally, provides an insight view to study the effect of various load into the lumbar spine with assignation of materials (Silva & Claro 2015; Kim et al. 2014; Schmidt et al. 2007; Denoziere & Ku 2006; Lu et al. 2014). The FE study was used to determine the shear and compression outcomes of the IVD between L4 to L5 to enhance the rehabilitation and prosthesis technology (Schmidt et al. 2013). Likewise, the speed of simulation on the complex model can be enhanced by using high performance computer. The persistently simulation and investigation of FEA on the lumbar spine model can enhance the understanding of its biomechanical effect under various type and group of prosthesis.

2.6.1 Material properties of the human lumbar spine

The vertebral body consists of cortical and cancellous bones. Moreover, the average thickness of cancellous and cortical bones are estimated to 0.35 mm and 0.5 mm in the lumbar spine region (Denoziere & Ku 2006). The mechanical properties of the bone structures are frequently assumed as isotropic elastic material in the lumbar spine (Kim et al. 2014; Schmidt et al., 2007; Rohlmann et al. 2009).

The IVD is comprises of nucleus pulposus (NP), annulus fibrosus (AF) and annulus fibers (Kim et al. 2014). The IVD enable the lumbar spine to withstand sudden forces from the kinematic motion. The mechanical behavior of the IVD is assumed to be incompressible when reacting with the load (Kim et al. 2015). Likewise, the most recommended way to illustrate the incompressible material behavior of IVD is assigning Mooney-Rivlin model in simulation (Schmidt et al. 2007; Kim et al. 2014; Park et al. 2013).

The facet joint is made up of superior and inferior processes of two adjacent vetebral body. It ensures lumbar spine under stable state when torsional force is applied (Kim et al. 2014). In the simulation process, the contact surface is normally assumed to be surface-to-surface contact elemtents by ignoring the existence of friction (Schmidt et al. 2007).

Generally, the ligaments of the lumbar spine are modeled as spring element (Rohlmann et al. 2009; Schmidt et al. 2007) or truss element (Kim et al. 2014) which are connected at the FE lumbar spine model.

Furthermore, the material properties of each part of the FE lumbar spine model have been set up according to their mechanical behavior. The material properties assignation in previous studies are shown in Table 2.2.

Table 2.2 The assignation of material properties for FE lumbar spine model in previous studies

Source	Cortical bone	Cancellous bone	Annulus fibrosus	Nucleus Pulposus	Annulus fibers	Ligament	Cartilage of Facet Joint	Solver
Park et al. (2013)	E = 12000 MPa ν= 0.3	E = 100 MPa ν= 0.2	Hyperelastic Mooney-Rivlin $C_1 = 0.18$ $C_2 = 0.045$	Incompressible fluid-filled cavity	Non-linear dependent on distance from disc centre, 6 layers criss-cross pattern	Non-linear stress strain curve	Hard frictionless contact, E = 11 MPa, $\nu = 0.4$, Initial gap = 0.5 mm	Abaqus 6.10 (SIMULIA Inc, Providence, Rhode Island, USA)
Rohlmann et al. (2007)	E = 10000 MPa $\nu = 0.3$ $E_1 = 22000$ MPa	$E_1 = 200$ MPa $E_2 = 140$ MPa $\nu_1 = 0.45$ $\nu_2 = 0.315$	Hyperelastic Neo-Hookean $C_1 = 0.3448$ $C_2 = 0.3$	Incompressible fluid-filled cavity	Non-linear dependent on distance from disc centre, 14 layers criss-cross pattern	Non-linear stress strain curve	Soft frictionless contact, Initial gap = 0.5 mm	Abaqus 6.10 (SIMULIA Inc, Providence, Rhode Island, USA)
Schmidt et al. (2007)	$E_2 = 11300$ MPa $\nu_1 = 0.484$ $\nu_2 = 0.203$	$E_1 = 200$ MPa $E_2 = 140$ MPa $\nu_1 = 0.45$ $\nu_2 = 0.315$	Hyperelastic Mooney-Rivlin $C_1 = 0.56$ $C_2 = 0.14$	Incompressible fluid-filled cavity	Non-linear stress- strain curve, 16 layers criss-cross pattern	Non-linear stress strain curve	Hard frictionless contact, E = 35 MPa, $\nu = 0.4$, Initial gap = 0.4 mm	Abaqus 6.10 (SIMULIA Inc, Providence, Rhode Island, USA)

Table 2.2 The assignation of material properties for FE lumbar spine model in previous studies (continued)

Source	Cortical bone	Cancellous bone	Annulus fibrosus	Nucleus Pulposus	Annulus fibers	Ligament	Cartilage of Facet Joint	Solver
Kim et al., (2014)	E_1 = 22000 MPa E_2 = 11300 MPa ν_1 = 0.484 ν_2 = 0.203	E_1 = 200 MPa E_2 = 140 MPa ν_1 = 0.45 ν_2 = 0.315	Solid E = 4.2 MPa ν = 0.45	Incompressible fluid-filled cavity	Non-linear stress- strain curve, 8 layers criss-cross pattern	Non-linear stress strain curve	Hard frictionless contact, E = 35 MPa, ν = 0.4, Initial gap = 0.5 mm	Abaqus 6.6 (SIMULIA Inc, Providence, Rhode Island, USA)

2.7 Finite element studies for human lumbar spine

The kinematic motion of the lumbar spine can be illustrated in 3 rotational and 3 translational motion (Panjabi et al. 1994). The three rotation motions stated are flexion-extension, lateral bending and axial rotation of the spine.

2.7.1 Range of Motion

The range of motion (ROM) is the measured constraint when the lumbar spine undergoes various rotation motion and it is indicated in term of angle (Kim et al. 2015; Li et al. 2009). However, the ROM illustrates the kinematic motion of the lumbar spine which can demonstrate the motion difference between normal spine and injured spine (Li et al. 2009). The trend of ROM in FE healthy lumbar spine model pattern is vitally important to be investigated to obtain the accurate result in future studies.

2.7.2 Intradiscal pressure of the nucleus pulposus

The magnitude of intradiscal pressure (IDP) of IVD plays an important role in predicting the loading condition of the FE lumbar spine model (Sato et al. 1999). The standing posture is frequently recommended to replace sitting posture in daily life. The reason is sitting posture tends to rise the pressure of NP nearly 40 % compared to standing posture (Wilke et al. 1999). However, the spine specialist concludes that the IDP of disc lumbar spine is incomparable to the other spine such as thoracic, cervical, sacrum, coccyx region due to different biomechanical environment (Polga et al. 2004). Thus, the verification of the lumbar spine uses the IDP of healthy IVD in vitro studies to validate the reliability of FE lumbar spine model for further simulation purposes (Markolf & Morris 1974; Ranu 1990).

2.7.3 Stress analysis of the annulus

Generally the DDD is normally declared as the causes of LBP. Therefore, the stress changes in the annulus in the IVD has significant effect on the biomechanical properties on the lumbar spine (Ruberte et al. 2009). In FE studies, the assignation of material properties of the disc is controlled to reduce the disc height that include severe disc degeneration on the lumbar spine simulation (Rohlmann et al. 2006). The reason is defected disc that comprises of weak annulus unable to receive extra compression normally from the body reduces the height of disc and can cause catastrophes effect to the other part of the lumbar spine (Palepu et al. 2012). Otherwise, the stresses exist in the center of the disc were predicted to be the greatest for the normal IVD (Rohlmann et al. 2006). Therefore, stress analysis in the annulus is vitally essential to be carried out to reduce the risk of disc dehydration.

2.8 Summary

However, the increasing trend of obesity population in the world exerted external load on the lumbar spine and capable to reduce the biomechanical properties of the IVD which causes low back pain. Likewise, the biomechanical effect of IVD at various human weight is worth to be investigated and studied using FEA at various BMI.

CHAPTER 3

MATERIALS AND METHODS

3.1 Overview

This chapter illustrates the methods and procedures implemented to develop FE model of human lumbar spine and validated through the verification from previous studies. The verified FE model was then simulated to investigate the biomechanical effects of IVD with various human weight. The flow chart for this study is shown in Figure 3.1.

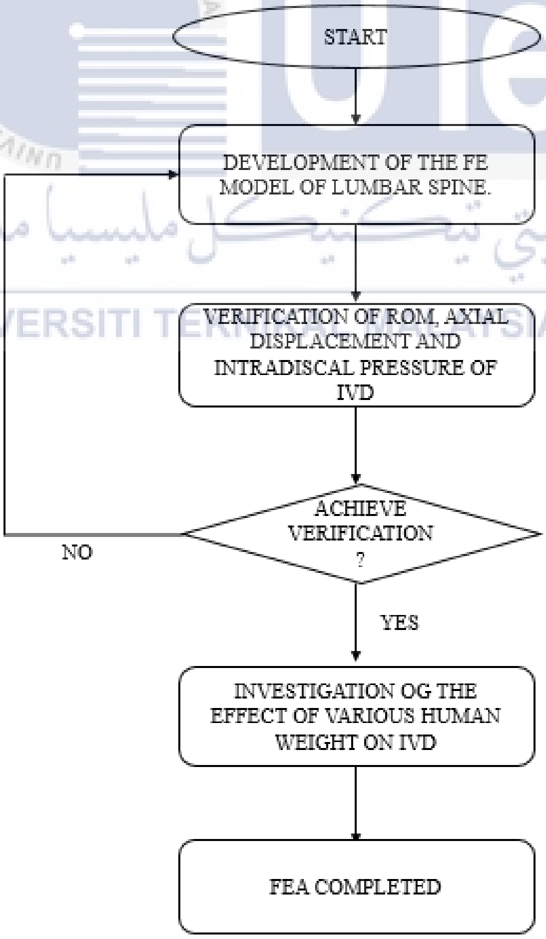

Figure 3.1 The flow chart of the methodology.

3.2 Finite element model of the lumbar spine

The FE lumbar spine model obtained from the Faculty of Biosciences and Medical Engineering UTM is simulated using ABAQUS. This lumbar spine is originated from male volunteer which is 21 years old, 173cm height and 70 kg weight which equivalent to BMI of 23.4. The FE lumbar spine model is developed using finite element software of ABAQUS 14.0 for verification and biomechanical effect purposes as shown in Figure 3.2.

Figure 3.2 The FE model of lumbar spine.

3.3 Material properties assignation of FE lumbar spine

The assignation of FE model's material properties is one of the criteria to yield precise and accurate biomechanical effect of lumbar spine. The list of material properties used in this FE model was shown in Table 3.1.

Table 3.1 The list of material properties of the FE model

Parts	Material properties	Reference
Cortical bone	E = 12000 MPa, v = 0.3	(Park et al. 2013)
Cancellous bone	E = 100 MPa, v = 0.2	(Park et al. 2013)

Articular cartilage	E = 35 MPa, v = 0.4	(Kim et al. 2014)
Nucleus pulposus	E = 1.0 MPa, v = 0.4999	(Schmidt et al. 2007)
Annulus ground substance	E = 4.2 MPa, v = 0.45	(Schmidt et al. 2007)

3.4 Verification of the finite element model

The verifications of the FE model were executed in term of intersegmental rotation of the lumbar spine and compression of IVD. However, the difference of geometry structure of FE with real human lumbar spine and material properties assignation tend to influence the reliability of the model (Xiao et al. 2010) .Otherwise, the verified results determines the accuracy of the FE lumbar spine model to operate in vivo studies. The verification results from the FE model are compared with the vitro experiment result to ensure it is developed with minimum difference in real condition (Jones & Wilcox 2008). The verification must be succeeded before further simulation of biomechanical effect of lumbar spine in various human weight are investigated.

3.4.1 Intersegmental rotations of the lumbar spine

The ROM of FE model was compared with previous studies under pure moment of 7.5 Nm for flexion extension (Panjabi et al. 1994). This verification aims to ensure stability of the FE model. The equation of the moment yields the force couple magnitude in Table 3.2 as shown in Equation (1) (Nordin & Frankel. 2001).

$$M = F \times d$$

Where M is the moment, F is the resultant force and d is the distance between anterior and posterior vertebral body. The equation of moment was further expanded to determine Fy and Fz as shown below:

$$F = \frac{7.5\ Nm}{0.03\ m}$$

$$F = 250\ N$$

Since $F = \sqrt{Fy^2 + Fz^2}$

Let Fy = 0.3 Fs (30 % of force acting on y-axis)

And Fz = 0.7 Fs (70 % of force acting on z-axis)

$$250 = \sqrt{(0.3Fs)^2 + (0.7Fs)^2}$$

Fs = 328 N

Therefore;

Fy = 98 N

Fz = 230 N

Table 3.2 The magnitude of force in y and z direction on the FE model

Loading direction	Anterior point		Posterior point	
	Fy (N)	Fz (N)	Fy (N)	Fz (N)
Flexion	-98	-230	98	230
Extension	98	230	-98	-230

Moreover, all nodes at the bottom surface of L5 vertebrae body were constrained in all direction which representing the boundary condition of the model. However, the loadings were set at the upper surface of L1 vertebrae in posterior and anterior point. The loading and boundary condition of the FE model in ROM verification in ABAQUS was shown in Figure 3.3.

Figure 3.3 The loading and boundary condition of the FE lumbar spine model in extension moment.

3.4.2 Compression of IVD

The varication of IVD was validated by comparing the IDP and axial displacement of IVD to the previous studies (Markolf & Morris 1974; Ranu 1990). Moreover, the FE model is exerted with the axial compression load to determine the relationship between the axial compressive laod with displacement as these two parameters are highly correlated (Xiao et al. 2010). Furthermore, the The upper surface of the L4 vetebrae was subjected to 1100 N vertical compressive load and the the bottom surface of L5 vetebrae was set as boundary condition by limiting the rotation and translation as shown in Figure 3.4.

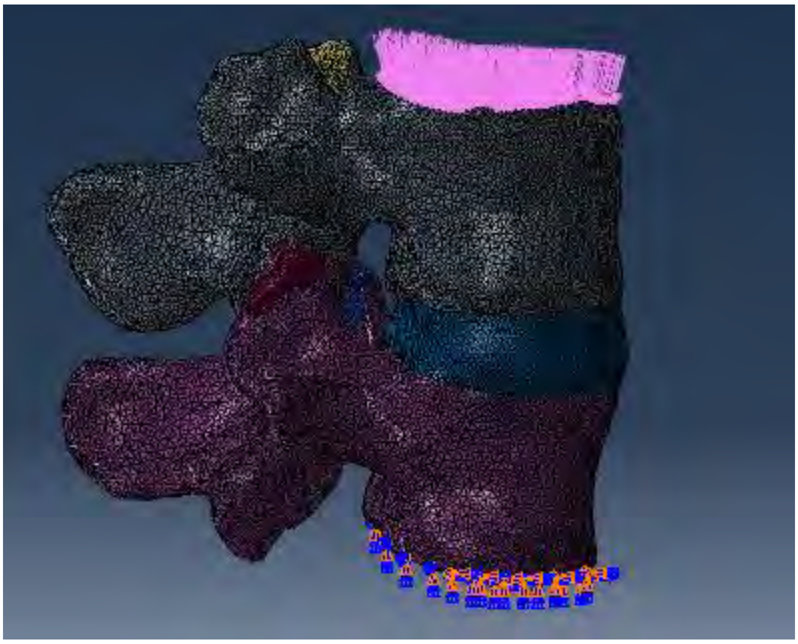

Figure 3.4 The loading and boundary condition of L4-L5 FE model in IVD verification.

3.5 Finite element analysis of the lumbar spine model at various human weight

The approximate 60 % of the human weight contributes to the compressive force in the lumbar spine (Kurutz & Oroszvary 2010). The various human weight comprise of normal weight, overweight and obesity with 55 kg, 80 kg and 110 kg (Walpole et al. 2012). The external load of 200 N from muscle effect is added in the weight of 500 N, 700 N and 900 N in the intersegmental rotations of the FE model (Rohlmann et al. 2009). Nevertheless, the compressive load of 700 N, 900 N and 1100 N will be implemented in the simulation to investigate the biomechanical effect of lumbar spine model.

CHAPTER 4

RESULT S AND DISCUSSION

4.1 Overview

This chapter discusses the results obtained from the lumbar spine models simulation. The verification of the finite element model is validated to assure the results are trustworthy. Furthermore, it is followed by the biomechanical effects of various human weight on the finite element model.

4.2 Verification of the L1-L5 lumbar spine model

The verification of the FE model was necessary to be executed on the flexion and extension motion of the lumbar spine, disc axial displacement and nucleus IDP of IVD. The verification process of the FE model is crucial to be carried out to replicate similar lumbar spine movement behavior.

4.2.1 Intersegmental Rotation of lumbar spine

The FE model of L1-L5 lumbar spine was verified in term of flexion and extension's ROM at pure moment of 7.5 Nm (Panjabi et al. 1994). The simulation of the FE model of lumbar spine shows comparable and curve trend with previous results as shown in Figure 4.1 (Panjabi et al. 1994). The percentage difference of the ROM in flexion reached 23.7 % at 7.5 Nm. The significant percentage difference of ROM was detected between 5 Nm, 2.5 Nm and -2.5 Nm, the percentage difference of the ROM was increased to 2.2 % when reaching -7.5 Nm. The most significant range of motion occurred during flexion was caused by the missing of ligaments which influenced the intersegmental rotation of the lumbar spine (Zander et al. 2004).

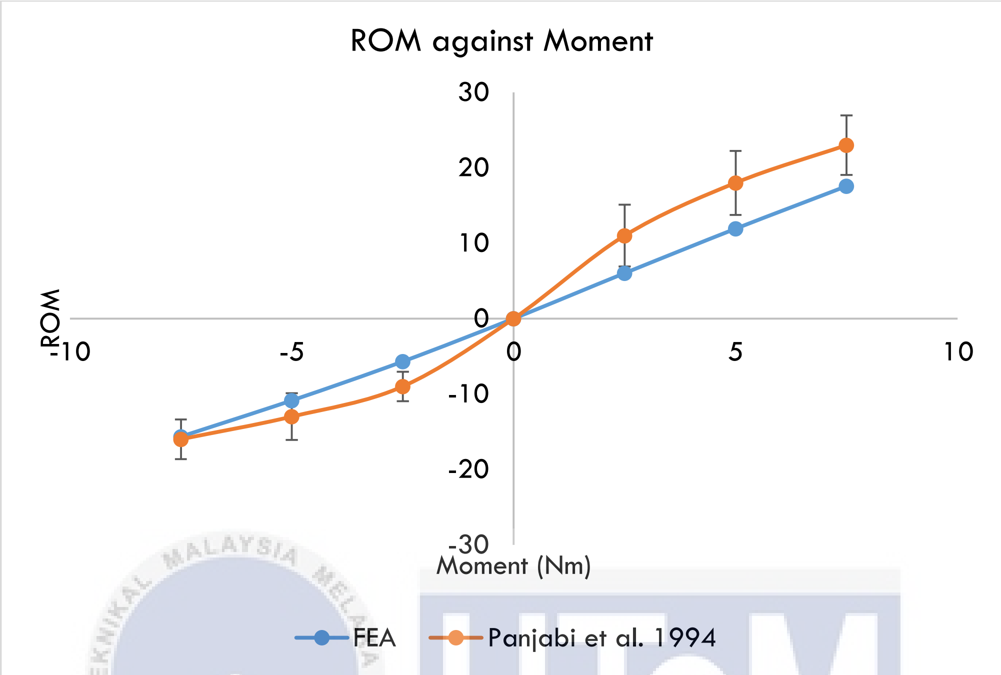

Figure 4.1 The comparison of total ROM of the lumbar spine between FE model and previously published paper result (Panjabi et al. 1994) under pure moment from –7.5 Nm to 7.5 Nm.

According to the ROM result simulated from the FE model, the FE model could yield reliable flexion and extension motion of the lumbar spine expecially when the motion reached to -7.5 Nm.

4.2.2 Intervertebral Disc

The axial displacement and IDP of the FE IVD shows comparable trend with previous studies as shown in Figure 4.2 and Figure 4.3 (Markolf & Morris. 1974; Ranu. 1990).The percentage difference of axial displacement and IDP of the IVD with previous studies revealed 22.3 % and 1.1 % under compressive load of 1100 N. The most significant of the axial displacement was caused by the anterior longitudinal ligaments constraint which capable to restrict the deformation of IVD in the largest compressive load (Marchi et al. 2012). According to the FE studies, the future results obtained from this FE model is capable to produce accurate axial displacement trends and future analysis using computational method.

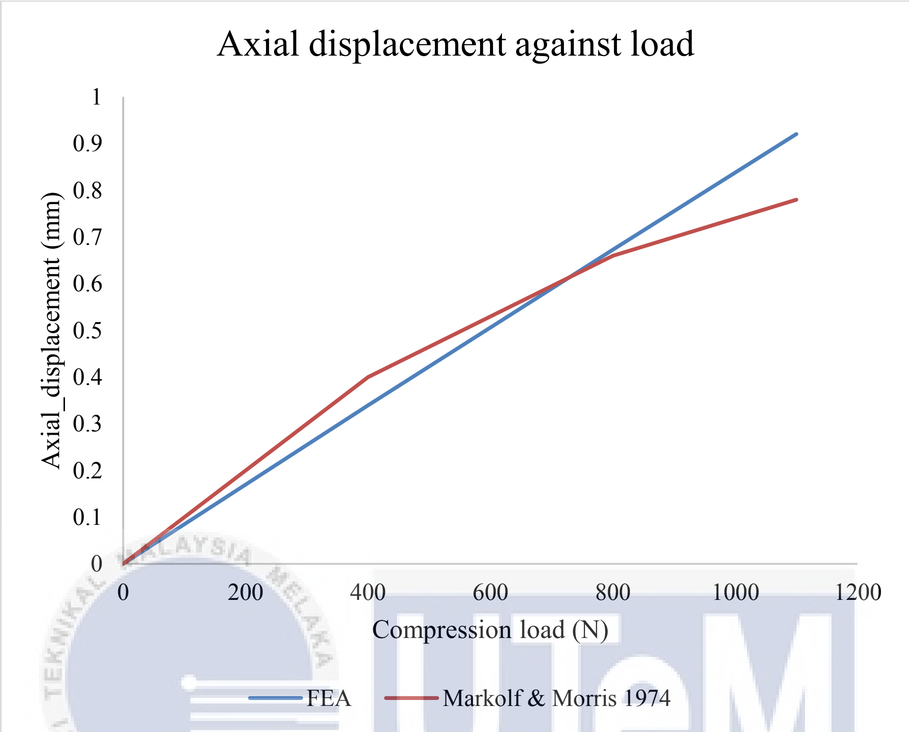

Figure 4.2 Comparison of FE model and previous studies of the IVD axial displacement under 1100 N.

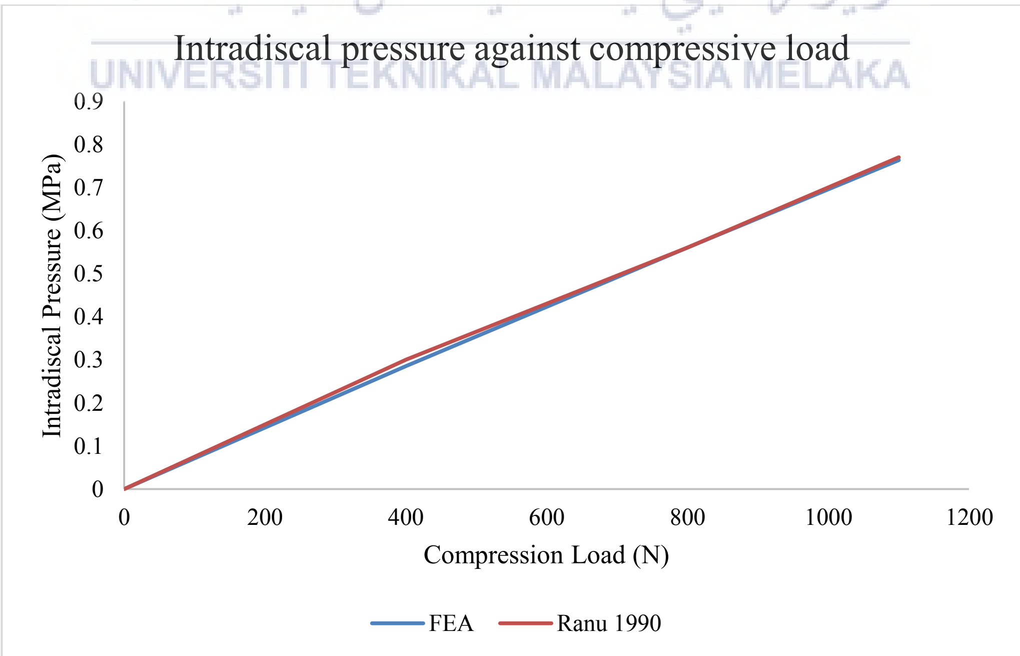

Figure 4.3 Comparison of FE model and previous studies of the IVD intradiscal pressure under 1100 N.

4.3 Biomechanical effect of IVD of various human weight on FE model

The biomechanical effect of normal, overweight and obesity on the IVD was analyzed under intersegmental rotation of the verified FE human lumbar spine model. However, the biomechanical effect of IVD can be divided into intradiscal pressure in nucleus pulposus and VMS in annulus fibrosus.

4.3.1 The intradiscal pressure of nucleus pulposus under various human weight.

The intradiscal pressure of nucleus pulposus of normal weight, overweight and obese under flexion and extension motion are illustrated in Figure 4.4 and Figure 4.5. The highest intradiscal pressure of nucleus pulposus occurs in the L2-L3 segment under combination of obese compressive load and extension motion with 2.70 MPa. Meanwhile, the segment of L1-L2 shows lowest intradiscal pressure of nucleus pulposus with 1.27 MPa under flexion motion and exerted with obese compressive load.

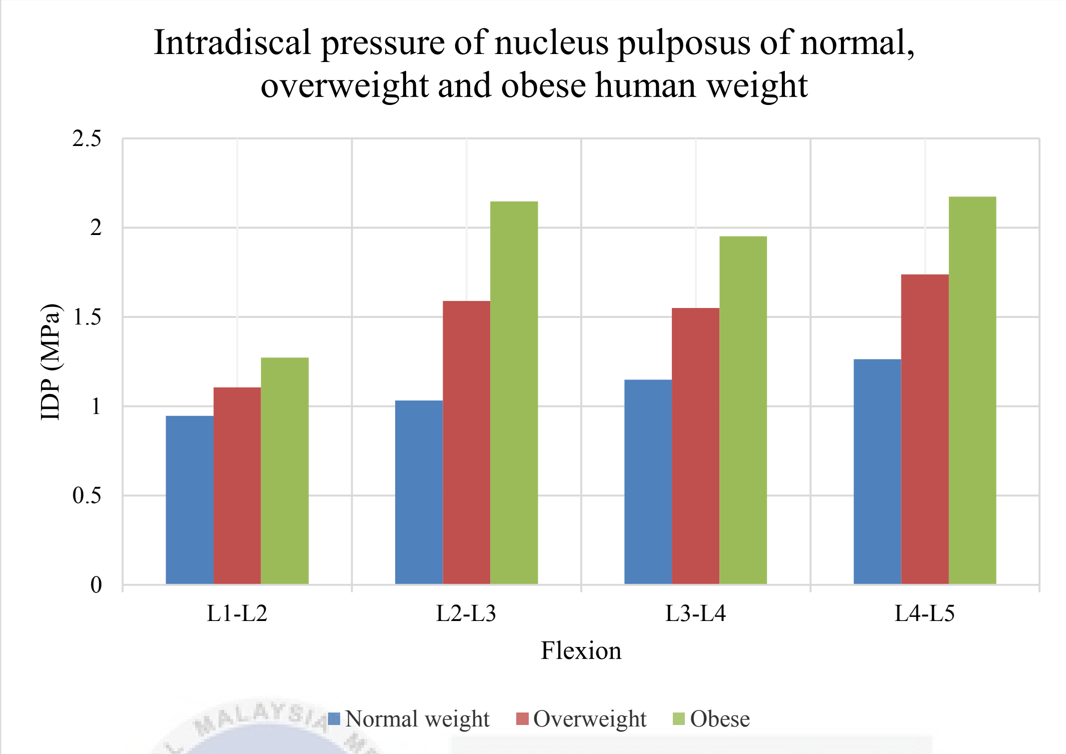

Figure 4.4 The intradiscal pressure of nucleus of normal, overweight and obese under flexion motion.

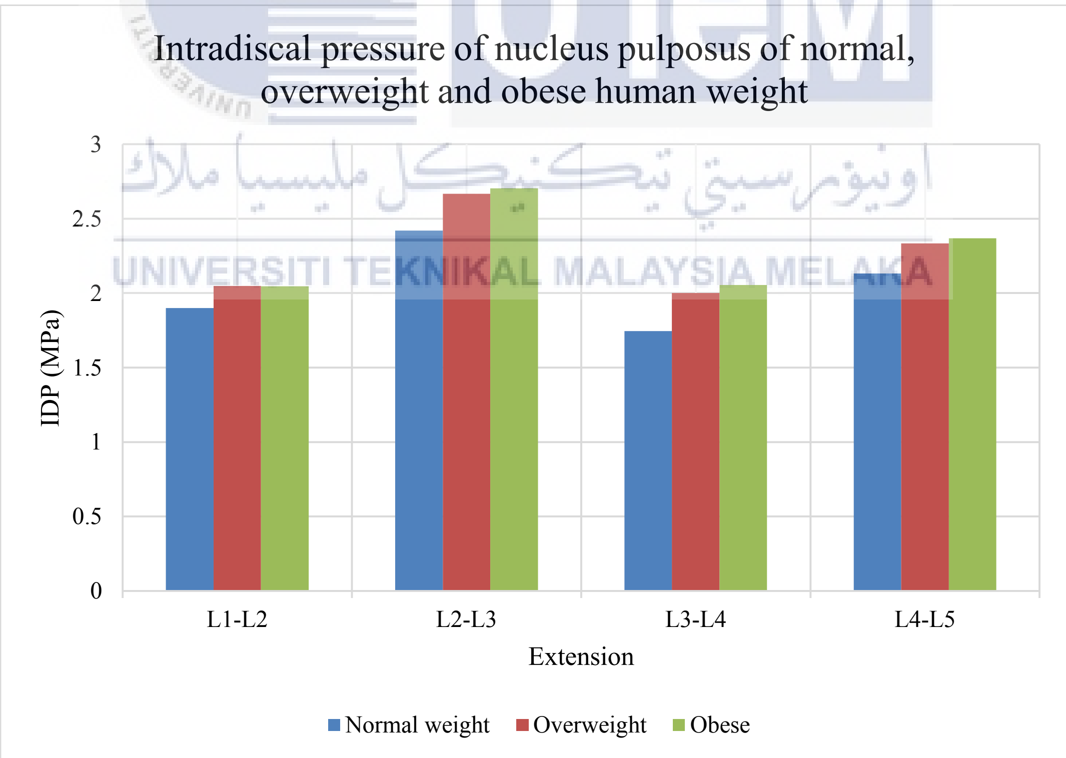

Figure 4.5 The intradiscal pressure of nucleus of normal, overweight and obese under extension motion.

Additionally, increasing trend of IDP in nucleus pulposus was shown under flexion and extension motion. However, there was significant difference presented in L2-L3 and L3-L4 segment in flexion and extension motion. Moreover, the intradiscal pressure of nucleus pulposus under overweight and obese in L2-L3 segment were 53.8 % and 107.7% greater than normal weight. Nevertheless, extension motion resulted difference with 14.7 % and 17.7 % in L3-L4 segment.

Furthermore, the IDP trend of L1-L2, L2-L3 andL3-L4 segment in flexion motion tend to shows comparable trend of healthy disc to degenerative disc which were 16.9-34.7 %, 53.8-107.7 % and 34.9-69.8 % (Park et al. 2013). Therefore, the non-symmetrical stress distribution in IVD tends to elevate the IDP in nucleus resulted in disc dehydration (Urban & Roberts 2003).

4.3.2 The annulus fibrosus stress of IVD under various human weight

The highest VMS of annulus fibrosus resulted during extension motion which was 3.10 MPa in L2-L3 segment when exerted to obese load as shown in Figure 4.7. Nonetheless, the lowest VMS of annulus fibrosus observed during flexion motion was 1.56 MPa in L1-L2 segment under obese compression loading as shown in Figure 4.6. Otherwise, the biggest difference during flexion motion was occur in L2-L3 segment which up to 53 % and 108.12 % higher than normal weight loading condition and the L3-L4 segment in extension motion resulted 13.3 % and 15.3 % greater than normal weight.

Other than L2-L3 segment in flexion, the difference of other segments resulted 5.74-11.50 %, 34.7-69.5 % and 32.6-61.3 % compared to normal weight condition. In extension motion, difference lumbar segment other than L3-L4 segment were 7.9-7.8 %, 9.9-11.2 % and 8.7-11 % respectively compared normal weight loading.

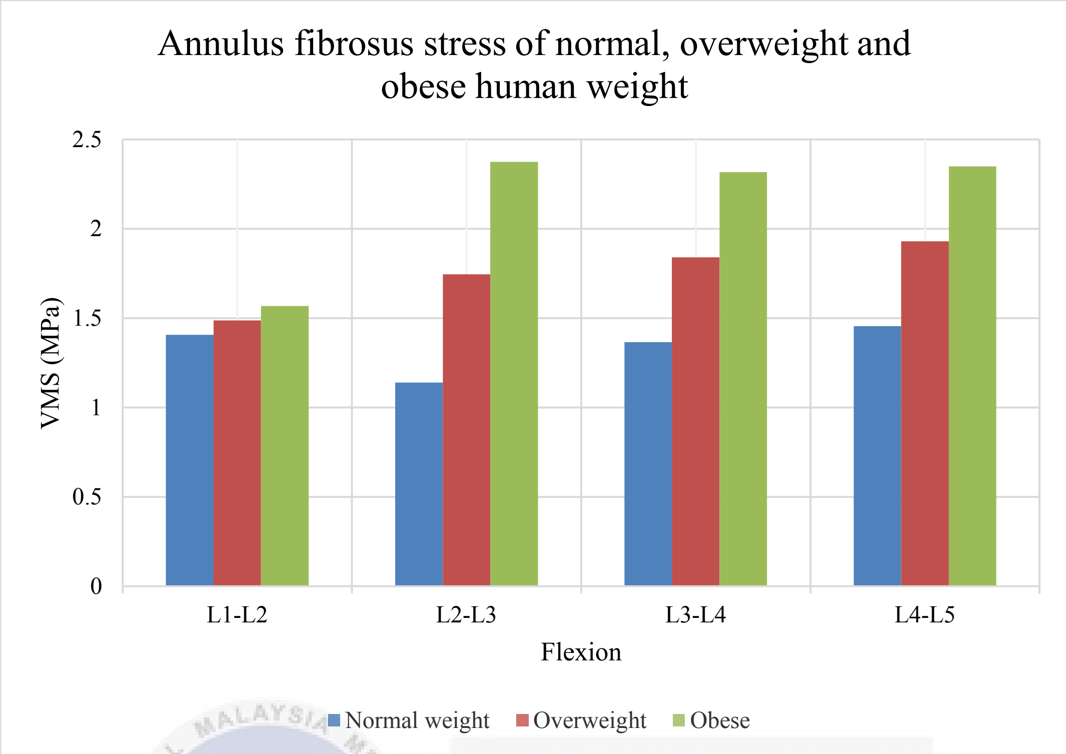

Figure 4.6 The annulus fibrosus stress under normal, overweight and obese human weight in flexion motion.

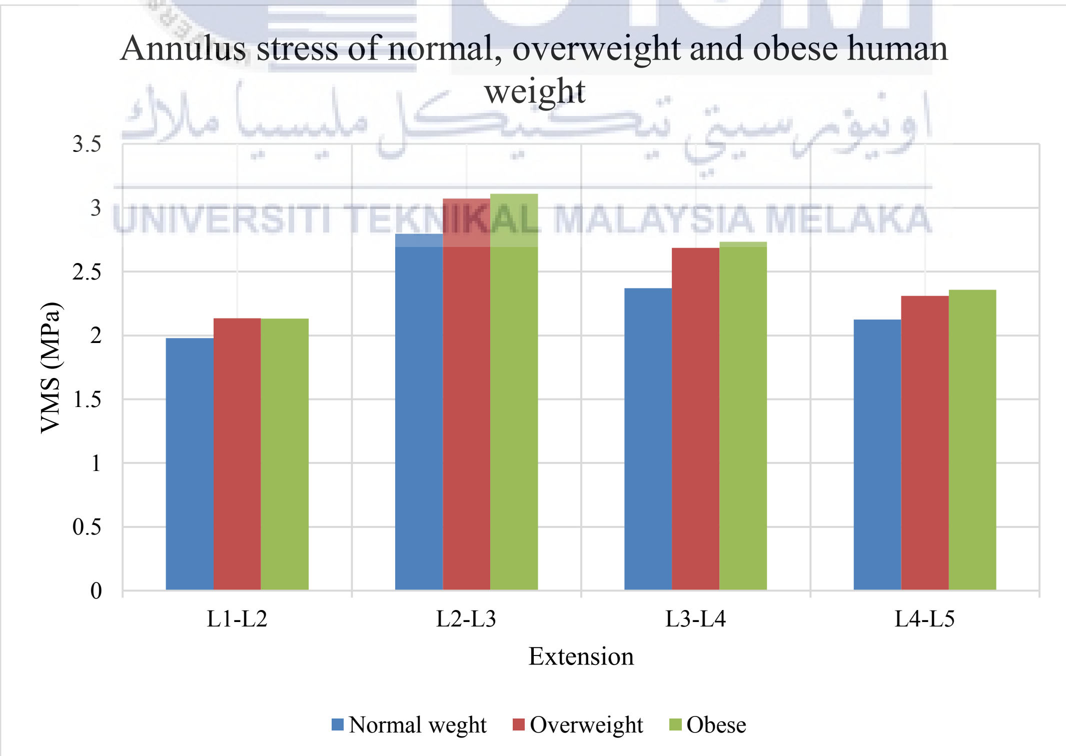

Figure 4.7 The annulus fibrosus stress under normal, overweight and obese human weight in extension motion.

The stress distribution in annulus fibrosus under various human weight during flexion and extension motion were illustrated in Figure 4.8 and Figure 4.9. It can be summarized that the annulus fibrosus increases in the heavier human weight in intersegmental rotation of lumbar spine. The increases of stress in annulus fibrosus will elevates the risk for the disc to undergo dehydration and rupture easily (Adams et al. 1996). The increasing trend of VMS of annulus fibrosus intended affect the morphological structure of the IVD and caused LBP (Evans & Sun 2006).

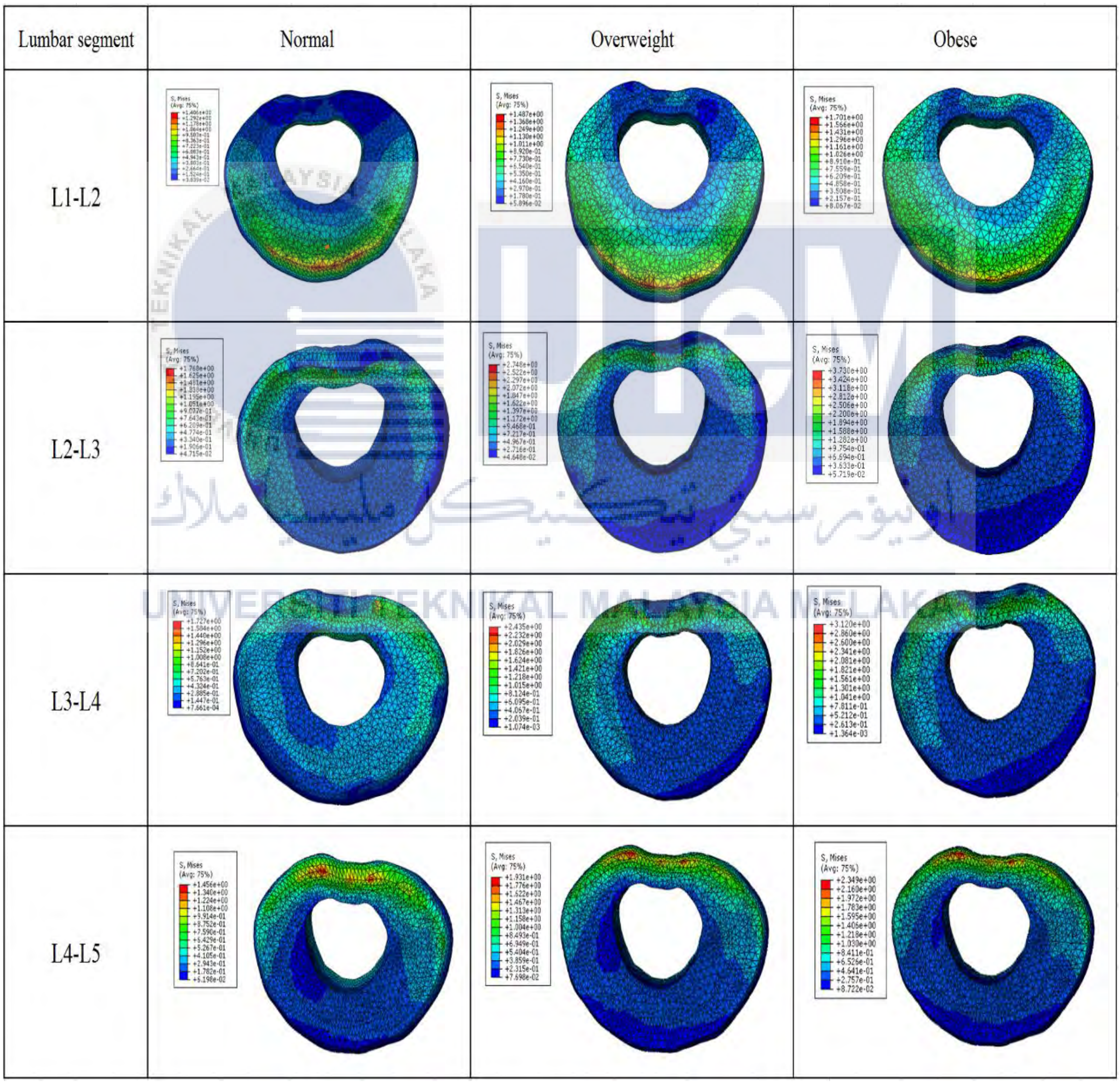

Figure 4.8 The stress distribution in the nucleus pulposus under normal, overweight and obese in flexion.

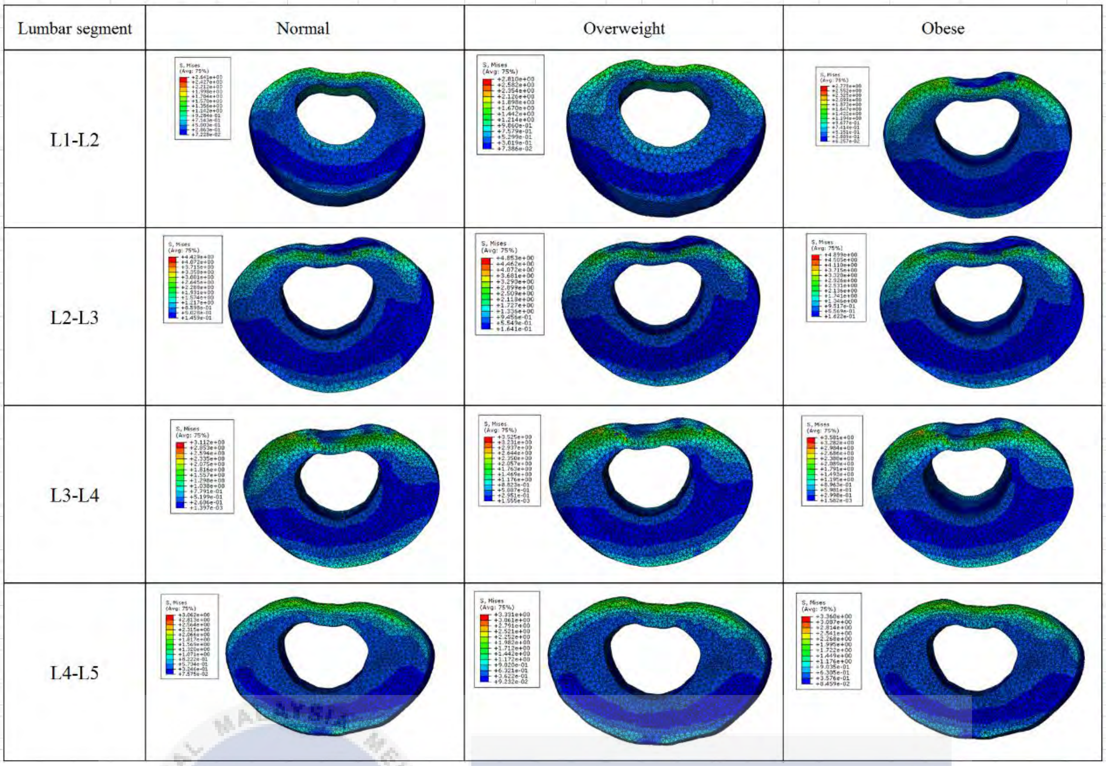

Figure 4.9 The stress distribution in the nucleus pulposus under normal, overweight and obese in extension.

.

CHAPTER 5

CONCLUSIONS AND RECOMMENDATION

5.1 Conclusion

This project aims to investigate the biomechanical effect of IVD by using FE model under various human weight. A validated FE lumbar spine model presently produced reliable and accurate result in the lumbar spine model especially in term of kinematic motion, stress distribution and intradiscal pressure. Therefore, the effect of normal, overweight and obese on the IVD can be analyzed during intersegmental rotation. Throughout the studies, obese population has higher risk to face LBP as the increasing trend of stress and pressure distribution in IVD which lead to DDD.

5.2 Recommendation for future studies

This FE model can be improved by changing the elastic properties of the IVD to hyperelastic properties. This properties is expected to provide better trend of range of motion against flexion and extension motion. Furthermore, the ligaments with specific properties and area are encouraged to be included in the FE model so that the stress distribution of whole lumbar spine model can be more equivalent and accurate. Otherwise, these two factor is crucial future research such as prosthesis that highly rely on the reliability of this FE lumbar spine model. Nevertheless, the future studies should include the other motion such as lateral bending and axial rotation in IVD so that all motion is taken seriously in analysis.

REFRENCES

Adams, M. A. (2004). Biomechanics of back pain. *Acupuncture in medicine*, *22*(4), 178-188. Retrieved October 10, 2016

Adams, M. A., McNally, D. S., & Dolan, P. (1996). 'STRESS'DISTRIBUTIONS INSIDE INTERVERTEBRAL DISCS. *J Bone Joint Surg Br*, *78*(6), 965-972.

Araújo, A., Peixinho, N., Pinho, A., & Claro, J. C. P. (2015, February). Comparison between the dynamic and initial creep response of porcine and human lumbar intervertebral discs. In *Bioengineering (ENBENG), 2015 IEEE 4th Portuguese Meeting on* (pp. 1-6). IEEE.

Bergmark, A. (1989). Stability of the lumbar spine: a study in mechanical engineering. *Acta Orthopaedica Scandinavica*, *60*(sup230), 1-54.

Denozière, G., & Ku, D. N. (2006). Biomechanical comparison between fusion of two vertebrae and implantation of an artificial intervertebral disc. *Journal of biomechanics*, *39*(4), 766-775.

Djurasovic, M., Bratcher, K. R., Glassman, S. D., Dimar, J. R., & Carreon, L. Y. (2008). The effect of obesity on clinical outcomes after lumbar fusion. *Spine*, *33*(16), 1789-1792.

Evans, P. J., & Sun, W. (2006, April). Finite element analysis and computer aided tissue engineering design of a replacement lumbar intervertebral disc. In *Bioengineering Conference, 2006. Proceedings of the IEEE 32nd Annual Northeast* (pp. 75-76). IEEE.

Ferguson, S. J., & Steffen, T. (2003, September 9). Biomechanics of the aging spine. *Eur Spine*, *12*(2), 97-103.

Fujiwara, A., Lim, T. H., An, H. S., Tanaka, N., Jeon, C. H., Andersson, G. B., & Haughton, V. M. (2000). The effect of disc degeneration and facet joint osteoarthritis on the segmental flexibility of the lumbar spine. *Spine*, *25*(23), 3036-3044.

Gordon-Larsen, P., Wang, H., & Popkin, B. M. (2014). Overweight dynamics in Chinese children and adults. *Obesity reviews*, *15*(S1), 37-48.

Han, K. S., Rohlmann, A., Yang, S. J., Kim, B. S., & Lim, T. H. (2011). Spinal muscles can create compressive follower loads in the lumbar spine in a neutral standing posture. *Medical engineering & physics*, *33*(4), 472-478.

Hussein, A. I., Mason, Z. D., & Morgan, E. F. (2013). Presence of intervertebral discs alters observed stiffness and failure mechanisms in the vertebra. *Journal of biomechanics*, *46*(10), 1683-1688.

Jaumard, N. V., Welch, W. C., & Winkelstein, B. A. (2011). Spinal facet joint biomechanics and mechanotransduction in normal, injury and degenerative conditions. *Journal of biomechanical engineering*, *133*(7), 071010.

Jones, A. C., & Wilcox, R. K. (2008). Finite element analysis of the spine: towards a framework of verification, validation and sensitivity analysis. *Medical engineering & physics*, *30*(10), 1287-1304.

Khalaf, K., Nikkhoo, M., Kuo, Y. W., Hsu, Y. C., Parnianpour, M., Campbell-Kyureghyan, N., ... & Wang, J. L. (2015, August). Recovering the mechanical properties of denatured intervertebral discs through Platelet-Rich Plasma therapy. In *Engineering in Medicine and Biology Society (EMBC), 2015 37th Annual International Conference of the IEEE* (pp. 933-936). IEEE.

Khan, M. F., Malik, A. S., Rozana, F., Xia, L., Nikkhoo, M., Wang, J. L., & Parnianpour, M. (2012, June). On low back pain: Identification of structural changes in system parameters for fatigue loaded intervertebral disc using PCA. In *Intelligent and Advanced Systems (ICIAS), 2012 4th International Conference on* (Vol. 1, pp. 378-381). IEEE.

Kim, H. J., Chun, H. J., Kang, K. T., Lee, H. M., Chang, B. S., Lee, C. K., & Yeom, J. S. (2015). Finite element analysis for comparison of Spinous process Osteotomies technique with conventional Laminectomy as lumbar decompression procedure. *Yonsei medical journal*, *56*(1), 146-153.

Kim, H. J., Kang, K. T., Chang, B. S., Lee, C. K., Kim, J. W., & Yeom, J. S. (2014). Biomechanical analysis of fusion segment rigidity upon stress at both the fusion and adjacent segments: a comparison between unilateral and bilateral pedicle screw fixation. *Yonsei medical journal*, *55*(5), 1386-1394.

Koes, B. W., Van Tulder, M. W., & Thomas, S. (2006). Diagnosis and treatment of low back pain. *British medical journal, 322*, 1430-1434.

Koh, J., Chaudhary, V., & Dhillon, G. (2010, March). Diagnosis of disc herniation based on classifiers and features generated from spine MR images. In *SPIE Medical imaging* (pp. 76243O-76243O). International Society for Optics and Photonics.

Kurtz, S. M., & Edidin, A. (2006). *Spine technology handbook.* Academic Press.

Kurutz, M. (2010). Finite element modelling of the human lumbar spine. *INTECH Open Access Publisher*, 209-236.

Kurutz, M., & Oroszváry, L. (2010). Finite element analysis of weightbath hydrotraction treatment of degenerated lumbar spine segments in elastic phase. *Journal of biomechanics*, *43*(3), 433-441.

Li, G., Wang, S., Passias, P., Xia, Q., Li, G., & Wood, K. (2009). Segmental in vivo vertebral motion during functional human lumbar spine activities. *European Spine Journal*, *18*(7), 1013-1021.

Loudon, J. K., Manske, R. C., & Reiman, M. P. (2012). *Clinical Mechanics and Kinesiology* (1st ed.). London: Human Kinetics.

Lu, Y., Maquer, G., Museyko, O., Püschel, K., Engelke, K., Zysset, P., ... & Huber, G. (2014). Finite element analyses of human vertebral bodies embedded in polymethylmethalcrylate or loaded via the hyperelastic intervertebral disc models provide equivalent predictions of experimental strength. *Journal of biomechanics*, *47*(10), 2512-2516.

Marchi, L., Oliveira, L., Coutinho, E., & Pimenta, L. (2012). The importance of the anterior longitudinal ligament in lumbar disc arthroplasty: 36-month follow-up experience in extreme lateral total disc replacement. *The International Journal of Spine Surgery*, *6*(1), 18-23.

Markolf, K. L., & Morris, J. M. (1974). The structural components of the intervertebral disc. *J Bone Joint Surg Am*, *56*(4), 675-687.

Martin, K., Fontaine, K. R., Nicklas, B. J., Dennis, K. E., Goldberg, A. P., & Hochberg, M. C. (2001). Weight loss and exercise walking reduce pain and improve physical functioning in overweight postmenopausal women with knee osteoarthritis. *JCR: Journal of Clinical Rheumatology*, *7*(4), 219-223.

Nabhani, F., & Wake, M. (2002). Computer modelling and stress analysis of the lumbar spine. *Journal of Materials Processing Technology*, *127*(1), 40-47.

Netter, F. H. (2006). *Atlas of Human Anatomy* (2nd ed.). Philadelphia: Saunders Elsevier.

Nordin, M., & Frankel, V. H. (2001). *Basic Biomechanics of the Musculoskeletal System* (3rd ed.). Philadelphia: Lippincott Williams & Wilkins.

Palepu, V., Kodigudla, M., & Goel, V. K. (2012). Biomechanics of disc degeneration. *Advances in orthopedics*, *2012*.

Panjabi, M. M. (2003). Clinical spinal instability and low back pain. *Journal of electromyography and kinesiology*, *13*(4), 371-379.

Panjabi, M. M., Oxland, T. R., Yamamoto, I., & Crisco, J. J. (1994). Mechanical behavior of the human lumbar and lumbosacral spine as shown by three-dimensional load-displacement curves. *The Journal of Bone & Joint Surgery*, *76*(3), 413-424.

Park, W. M., Kim, K., & Kim, Y. H. (2013). Effects of degenerated intervertebral discs on intersegmental rotations, intradiscal pressures, and facet joint forces of the whole lumbar spine. *Computers in biology and medicine*, *43*(9), 1234-1240.

Polga, D. J., Beaubien, B. P., Kallemeier, P. M., Schellhas, K. P., Lew, W. D., Buttermann, G. R., & Wood, K. B. (2004). Measurement of in vivo intradiscal pressure in healthy thoracic intervertebral discs. *Spine*, *29*(12), 1320-1324.

Porto, H. C., Pechak, C. M., Smith, D. R., & Reed-Jones, R. J. (2012). Biomechanical Effects of Obesity on Balance. *International Journal of Exercise Science, 5*(4), 301-320.

Ranu, H. S. (1990). Measurement of pressures in the nucleus and within the annulus of the human spinal disc: due to extreme loading. *Proceedings of the Institution of Mechanical Engineers, Part H: Journal of Engineering in Medicine*, *204*(3), 141-146.

Rohlmann, A., Zander, T., Rao, M., & Bergmann, G. (2009). Realistic loading conditions for upper body bending. *Journal of Biomechanics*, *42*(7), 884-890.

Rohlmann, A., Zander, T., Schmidt, H., Wilke, H. J., & Bergmann, G. (2006). Analysis of the influence of disc degeneration on the mechanical behaviour of a lumbar motion segment using the finite element method. *Journal of biomechanics*, *39*(13), 2484-2490.

Ruberté, L. M., Natarajan, R. N., & Andersson, G. B. (2009). Influence of single-level lumbar degenerative disc disease on the behavior of the adjacent segments—a finite element model study. *Journal of biomechanics*, *42*(3), 341-348.

Sato, K., Kikuchi, S., & Yonezawa, T. (1999). In vivo intradiscal pressure measurement in healthy individuals and in patients with ongoing back problems. *Spine*, *24*(23), 2468.

Schmidt, H., Bashkuev, M., Dreischarf, M., Rohlmann, A., Duda, G., Wilke, H. J., & Shirazi-Adl, A. (2013). Computational biomechanics of a lumbar motion segment in pure and combined shear loads. *Journal of biomechanics*, *46*(14), 2513-2521.

Schmidt, H., Kettler, A., Heuer, F., Simon, U., Claes, L., & Wilke, H. J. (2007). Intradiscal pressure, shear strain, and fiber strain in the intervertebral disc under combined loading. *Spine*, *32*(7), 748-755.

Schmidt, H., Kettler, A., Rohlmann, A., Claes, L., & Wilke, H. J. (2007). The risk of disc prolapses with complex loading in different degrees of disc degeneration–a finite element analysis. *Clinical Biomechanics*, *22*(9), 988-998.

Shiri, R., Karppinen, J., Leino-Arjas, P., Solovieva, S., & Viikari-Juntura, E. (2010). The association between obesity and low back pain: a meta-analysis. American journal of epidemiology, 171(2), 135-154.

da Silva, I. M., Claro, J. C. P., & Castro, A. P. (2015, February). Geometric sensitivity analysis of a lumbar motion segment FE model. In *Bioengineering (ENBENG), 2015 IEEE 4th Portuguese Meeting on* (pp. 1-7). IEEE.

Smith, L. J., Nerurkar, N. L., Choi, K. S., Harfe, B. D., & Elliott, D. M. (2011). Degeneration and regeneration of the intervertebral disc: lessons from development. *Disease models & mechanisms*, *4*(1), 31-41.

Tashtoush, A. (2015, October). Therapeutic Degenerative Disc Disease Using Disc Rehabilitation Table (DRT). In *Modelling Symposium (EMS), 2015 IEEE European* (pp. 51-56). IEEE.

Unal, Y., Kocer, H. E., & Akkurt, H. E. (2011, June). A comparison of feature extraction techniques for diagnosis of lumbar intervertebral degenerative disc disease. In *Innovations in Intelligent Systems and Applications (INISTA), 2011 International Symposium on* (pp. 490-494). IEEE.

Urban, J. P., & Roberts, S. (2003). Degeneration of the intervertebral disc. *Arthritis Res Ther,* *5*(3), 120-130.

Viera, E. R. (2008). *Biomechanics in Ergonomics* (2nd ed.). (S. Kumar, Ed.) New York: CRC Press.

Vismara, L., Menegoni, F., Zaina, F., Galli, M., Negrini, S., & Capodaglio, P. (2010). Effect of obesity and low back pain on spinal mobility: a cross sectional study in women. *Journal of neuroengineering and rehabilitation*, *7*(1), 3.

Walpole, S. C., Prieto-Merino, D., Edwards, P., Cleland, J., Stevens, G., & Roberts, I. (2012). The weight of nations: an estimation of adult human biomass. *BMC public health*, *12*(1), 439.

Wilke, H. J., Neef, P., Caimi, M., Hoogland, T., & Claes, L. E. (1999). New in vivo measurements of pressures in the intervertebral disc in daily life. *Spine*, *24*(8), 755-762.

Wong, C., Gehrchen, P. M., Darvann, T., & Kiaer, T. (2003). Nonlinear finite-element analysis and biomechanical evaluation of the lumbar spine. *IEEE transactions on medical imaging*, *22*(6), 742-746.

Xiao, Z., Wang, L., Gong, H., Gao, J., & Zhang, X. (2010, October). Establishment and verification of a non-linear finite element model for human L4–L5 lumbar segment. In *Biomedical Engineering and Informatics (BMEI), 2010 3rd International Conference on* (Vol. 3, pp. 1171-1175). IEEE.

Zander, T., Rohlmann, A., & Bergmann, G. (2004). Influence of ligament stiffness on the mechanical behavior of a functional spinal unit. *Journal of biomechanics*, *37*(7), 1107-1111.

APPENDIX A

The raw data of verification of the lumbar spine model

Flexion

Moment	Part	Nodes (1,3)	Coord Y	Coord Z	Nodes (2,4)	Coord Y	Coord Z
0	L5	339	217.21	-386.7	28648	249.68	-378.5
	L1	5454	227.86	-225.3	1901	260.55	-232.4

Moment	Part	Nodes (1,3)	Coord Y	Coord Z	Nodes (2,4)	Coord Y	Coord Z
2.5	L5	339	217.21	-386.7	28648	249.68	-378.5
	L1	5454	220.4	-226.2	1901	253.83	-229.8

Moment	Part	Nodes (1,3)	Coord Y	Coord Z	Nodes (2,4)	Coord Y	Coord Z
5.0	L5	339	217.21	-386.7	28648	249.68	-378.5
	L1	5454	212.94	-227.1	1901	247.11	-227.3

Moment	Part	Nodes (1,3)	Coord Y	Coord Z	Nodes (2,4)	Coord Y	Coord Z
7.5	L5	339	217.21	-386.7	28648	249.68	-378.5
	L1	5454	205.48	-228	1901	240.4	-224.7

Extension

Moment	Part	Nodes (1,3)	Coord Y	Coord Z	Nodes (2,4)	Coord Y	Coord Z
0	L5	339	217.21	-386.7	28648	249.68	-378.5
	L1	5454	227.86	-225.3	1901	260.55	-232.4

Moment	Part	Nodes (1,3)	Coord Y	Coord Z	Nodes (2,4)	Coord Y	Coord Z
-2.5	L5	339	217.21	-386.7	28648	249.68	-378.5
	L1	5454	234.91	-224.4	1901	266.88	-234.7

Moment	Part	Nodes (1,3)	Coord Y	Coord Z	Nodes (2,4)	Coord_Y	Coord_Z
-5	L5	339	217.21	-386.7	28648	249.68	-378.5
	L1	5454	241.32	-223.5	1901	272.64	-236.9

Moment	Part	Nodes (1,3)	Coord Y	Coord Z	Nodes (2,4)	Coord_Y	Coord_Z
-7.5	L5	339	217.21	-386.7	28648	249.68	-378.5
	L1	5454	247.33	-222.7	1901	278.03	-238.9

Moment	z1	z2	y1	y2	z2-z1	y2-y1	m1	z3	z4	y3	y4	z4-z3	y4-y3	m2	Rom	Rom (rad	Rom (deg	Panjabi
-7.5002	-386.75	-378.48	217.214	249.683	8.274	32.469	0.25483	-222.68	-238.9	247.333	278.028	-16.222	30.695	-0.5285	-0.7357	-0.2732	-15.655	-16
-5.0002	-386.75	-378.48	217.214	249.683	8.274	32.469	0.25483	-223.54	-236.88	241.316	272.638	-13.333	31.322	-0.4257	-0.652	-0.1895	-10.857	-13
-2.5001	-386.75	-378.48	217.214	249.683	8.274	32.469	0.25483	-224.41	-234.73	234.908	266.884	-10.326	31.976	-0.3229	-0.5619	-0.0994	-5.6957	-9
0	-386.75	-378.48	217.214	249.683	8.274	32.469	0.25483	-225.29	-232.36	227.862	260.545	-7.067	32.683	-0.2162	-0.4625	0	0	0
2.50008	-386.75	-378.48	217.214	249.683	8.274	32.469	0.25483	-226.18	-229.8	220.4	253.829	-3.62	33.429	-0.1083	-0.3574	0.10508	6.02072	11
5.00015	-386.75	-378.48	217.214	249.683	8.274	32.469	0.25483	-227.08	-227.25	212.938	247.114	-0.173	34.176	-0.0051	-0.2546	0.20789	11.9111	18
7.50024	-386.75	-378.48	217.214	249.683	8.274	32.469	0.25483	-227.98	-224.7	205.476	240.398	3.274	34.922	0.0938	-0.156	0.30643	17.5571	23

Moment	Rom(deg)	Difference (%)	Moment	Panjabi	Error (deg)
-7.5	-15.65	-2.157	-7.5	-16	2.6382
-5	-10.86	-16.48	-5	-13	3.0806
-2.5	-5.696	-36.71	-2.5	-9	1.9494
0	0	0	0	0	0
2.5001	6.0207	-45.27	2.5001	11	4.089
5.0002	11.911	-33.83	5.0002	18	4.2379
7.5002	17.557	-23.66	7.5002	23	3.9357

L4_17130

Compressive load (N)	Axial displacement (mm)	Error (%)	Compression load (N)	Markolf (mm)
0	0	0	0	0
400	0.3397	-15.08	400	0.4
800	0.6728	1.9447	800	0.66
1100	0.9206	18.029	1100	0.78

L4-L5 nucleus propulsus_1191

Compressive load (N)	Intradiscal Pressure (MPa)	Error	Compressive load (N)	Ranu (MPa)
0	0	0	0	0
400	0.2851	-4.968	400	0.3
800	0.5604	0.0659	800	0.56
1100	0.7632	-0.883	1100	0.77

APPENDIX B

The raw data of the effect of human weight on the lumbar spine model

Flexion

IVD	VMS (MPa)				
	Normal	Overweight	Obese	Change of overweight (%)	Change of obese (%)
L1-L2	1.4062	1.487	1.5679	5.7474	11.498
L2-L3	1.1407	1.7449	2.3741	52.966	108.12
L3-L4	1.3663	1.8398	2.3164	34.66	69.54
L4-L5	1.4561	1.9306	2.3488	32.591	61.311

Extension

IVD	VMS (MPa)				
	Normal	Overweight	Obese	Change of overweight (%)	Change of obese (%)
L1-L2	1.979	2.1354	2.1327	7.9031	7.7687
L2-L3	2.7963	3.0732	3.1089	9.9043	11.181
L3-L4	2.3703	2.6851	2.7331	13.277	15.303
L4-L5	2.1239	2.3091	2.3575	8.7222	10.997

Flexion

IVD	IDP (MPa)				
	Normal	Overweight	Obese	Change of overweight (%)	Change of obese (%)
L1-L2	2.305	2.4175	2.5299	4.878	9.7561
L2-L3	2.1753	3.5711	4.9637	64.167	128.19
L3-L4	2.4925	3.6373	4.7295	45.933	89.751
L4-L5	3.1375	4.244	5.2027	35.268	65.825

Extension

IVD	IDP (MPa)				
	Normal	Overweight	Obese	Change of overweight (%)	Change of obese (%)
L1-L2	1.899	2.0485	2.0454	7.8743	7.7116
L2-L3	2.4196	2.6669	2.7041	10.221	11.756
L3-L4	1.7454	2.0004	2.0543	14.608	17.698
L4-L5	2.1325	2.3349	2.3689	9.4903	11.086